Rho-dependent Termination within the *trp t′* Terminator. I. Effects of Rho Loading and Template Sequence†

Anne Q. Zhu‡ and Peter H. von Hippel*

Institute of Molecular Biology and Department of Chemistry, University of Oregon, Eugene, Oregon 97403-1229

Received November 26, 1997; Revised Manuscript Received May 6, 1998

ABSTRACT: About one-half of the terminators of the *Escherichia coli* genome require transcription termination factor rho to function. Here we use the very "diffuse" *trp t′* terminator of *E. coli* to show that both template sequence and transcript secondary structure are involved in controlling the template positions and efficiencies of rho-dependent termination. Termination begins in the wild-type *trp t′* terminator sequence ∼97 bps downstream of the promoter under our standard reaction conditions, and termination efficiencies for individual positions on three related templates have been determined in the form of quantitative patterns of rho-dependent RNA release. Comparison of these patterns shows that the rho-dependent termination efficiency at individual template positions depends primarily on the nucleotide sequence at and near the putative 3′ end of the transcript, although these efficiencies can also be influenced by RNA sequence elements located further upstream. The amplitudes of the peaks of the RNA release patterns at specific template positions are controlled primarily by the effectiveness of the binding of the rho hexamer to the "rho loading site" of the transcript. Introduction of a stable element of secondary structure into the nascent RNA within the loading site both shifts the position of initial rho-dependent termination downstream and decreases the amplitudes of the peaks of the RNA release pattern at the corresponding sequences. These results and others are consistent with the view that rho-dependent terminators contain two essential components: (i) an upstream rho loading site on the RNA that is 70−80 nucleotide residues in length, essentially devoid of secondary structure, and which contains sufficient numbers of rC residues to activate the RNA-dependent ATPase of rho; and (ii) a downstream sequence within which termination actually occurs. In this study we use the *trp t′* terminator to characterize the involvement of each of these sequence components in detail in order to provide the parameters required to define a quantitative mechanistic model for the function of rho in transcript termination.

The *Escherichia coli* transcription termination factor rho is required to release RNA transcripts from transcription complexes at rho-dependent terminators located along the DNA template (*1*; for reviews see refs *2*−*4*). Rho-dependent termination can occur only after specific template sequences that code for a rho "loading site" have been transcribed into the nascent RNA. An effective rho loading site comprises a strong binding site for the rho hexamer and is characteristically 70−80 nts[1] in length, carries little or no stable secondary structure, and is relatively rich in cytosine residues (*5*−*7*). The loading of rho onto the nascent transcript activates the cryptic RNA-dependent ATPase activity of rho (*8*) and also its ATP-dependent and directional (5′ → 3′ along the RNA) RNA−DNA helicase activity (*9, 10*). RNA transcripts are released from elongation complexes that are paused downstream of a rho loading site when rho and ATP are present (*11*−*13*).

More than two decades of research have revealed much about the structure and function of the rho protein itself (for a summary see ref *14*). However, details of the mechanisms used by this protein to trigger RNA release have remained unclear. Early studies showed that many strong rho-dependent termination sites are also sites of lengthy transcription complex pausing in the absence of rho (*15*−*18*). More recent studies have suggested that rho functions within the context of a direct kinetic competition between rho and RNA polymerase, with the efficiency of rho-dependent termination at the *λtR1* terminator depending on the relative rates of transcript elongation by RNA polymerase and the ATPase activity of rho, with the latter activity being assumed to be proportional to the rate of rho movement along the nascent transcript (*19*). Underlying this kinetic competition mechanism was the implicit assumption that rho is thermodynamically capable of releasing RNA from any transcription complex that it could "catch up with" along the template (*12*), presumably by acting as a directional RNA−DNA helicase (*9*).

An apparent challenge to the simplest version of this kinetic competition model for rho action was posed by the demonstration that the recently discovered elongation factor, NusG, can increase the rate of transcriptional elongation (*20*)

† This research was supported in part by USPHS Research Grants GM-15792 and GM-29158 (to P.H.v.H.) and was submitted (by A.Q.Z.) to the Graduate School of the University of Oregon in partial fulfillment of the requirements for the Ph.D. degree in Chemistry. P.H.v.H. is an American Cancer Society Research Professor of Chemistry.

‡ Present Address: Howard Hughes Medical Institute, University of Chicago, Box MC1028 N125, Chicago, IL 60637.

* Corresponding author. E-mail: petevh@molbio.uoregon.edu.

[1] Abbreviations: nt(s), nucleotide residue(s); bp(s), base pair(s); NTP(s), nucleoside-5′-triphosphate(s); ApU, adenosine 3′-5′ uridine; β-ME, β-mercapto-ethanol; PCR, polymerase chain reaction.

S0006-2960(97)02911-5 CCC: $15.00
Published on Web 07/24/1998

and also appears to move the rho-dependent termination zone *upstream*, as well as increasing somewhat the overall efficiency of rho-dependent termination (*21, 22*). In addition, while the NusA protein of *E. coli* is known to decrease the rate of elongation (*16, 23, 24*) and to increase termination efficiency at intrinsic terminators (*25*), it also appears to shift the rho-dependent termination zone further *downstream* at the *λtR1* terminator (*26*) and at the *trp t′* terminators used in this study (A. Q. Zhu, unpublished data).

In this study we have used the *trp t′* terminator and its variants to examine the mechanism of rho-dependent termination. We chose this terminator as a model system because it has been well characterized by deletion and mutation studies (*27*−*32*), although it has not been subjected to detailed mechanistic examination. Also, it is a very "long" terminator, in that the termination zone is spread over more than 100 nts along the template. As a consequence, the effects of changes in template sequence and transcription conditions on termination position and termination efficiency can be examined over a range of potential template positions.

The *trp t′* terminator is located at the very end of the tryptophan operon of *E. coli* and lies downstream of the five contiguous structural genes of the polycistronic *trp* operon (*trp*A through E) and of the intrinsic *trp t* terminator (*33*). The *trp t′* terminator was originally identified when deletion of the sequence in which it occurs resulted in read-through from the *trp* operon in vivo (*27, 28*). Wu et al. (*29*) then subcloned the DNA sequence of 200 bps that spans the region over which deletion resulted in read-through. These authors showed that this terminator is completely rho-dependent and very efficient, although the observed termination endpoints appeared to be very heterogeneous and were spread over a template sequence of more than 100 bps. Comparable rho-dependent termination efficiencies were achieved in vivo and in vitro when a 211-bp version of this fragment was inserted between the *gal* promoter and the *gal*K reporter gene (*34, 31*), demonstrating that the function of the *trp t′* terminator is not promoter-specific. RNA transcripts of this 211-bp terminator were also shown to support rho-dependent RNA−DNA helicase activity and could be used by rho to remove complementary DNA oligomers annealed at the 3′ end of the transcript (*9, 10, 35, 36*).

As with other rho-dependent terminators, further dissection of *trp t′* revealed two distinct functional zones, comprising an essential upstream rho loading site that encodes all the signals for rho-dependent termination and a downstream termination region that contains all the endpoints of transcription. The first 105-bp region of this terminator was defined by Galloway and Platt (*30, 31*) as the rho "loading site" on the basis of deletion studies. The entire 211-bp terminator was later subjected to a deletion scan analysis to search for sequence-specific elements important for the in vitro rho-dependent termination function (*32*). A pair of elements within the "loading site" were identified as specific "rho utilization sites" and were called rutA and rutB. These sites shared certain sequence homologies with sites proposed to be essential for the activation of rho ATPase and hence for rho-dependent termination at the *λtR1* terminator (*37*). The *rut*B element of *trp t′* was reported to be more important since the *rut*A element alone was found to be nonfunctional in the absence of *rut*B (*32*). These authors also speculated that two repetitive elements, termed *R1* and *R2*, within the *trp t′* rho loading site might also be important for rho-dependent termination.

We show here that the template region over which rho-dependent termination is possible within the *trp t′* terminator is strongly dependent on the reaction conditions used, and that termination under certain conditions occurs within the previously defined rho loading site even before the putatively essential *rut*B sequence has been transcribed. The pattern of termination efficiency at individual positions is highly dependent on the local template sequence but can be altered by changing the sequence between the template regions that code for the rho loading site and the transcript termination zone. The magnitude of the termination efficiency at individual positions seems to be affected by rho loading. The presence of RNA secondary structure within the rho loading site delays the start point of termination, but this effect can be relieved by destabilizing the secondary structure of the RNA by replacing guanosine with inosine residues within the transcript. Termination within an unrelated plasmid DNA sequence of approximately the same length as the wild type *trp t′* termination zone, inserted downstream of the rho loading site of *trp t′*, is shown to be highly heterogeneous in terms of template position, with an overall termination efficiency that is about 80% of that of the wild-type terminator under all reaction conditions tested.

Our results support the idea that recognition between rho and the nascent RNA transcript is only "pseudospecific", in that the general structureless nature of the rho loading site seems to be more important than any specific RNA sequence. We also show that a single rho hexamer can functionally load onto the transcript as soon as a sufficient length of unstructured template has been synthesized, and that this rho hexamer can move processively to induce rho-dependent termination along the *trp t′* terminator with an overall efficiency (per terminator) of close to 1.0 at the salt concentrations used in our standard assay. These results confirm that the loading of rho onto the nascent transcript is the determining step in rho-dependent termination and provide the background and some of the parameters needed for the general quantitative model of rho function in transcription termination that is developed in the companion paper (*38*).

MATERIALS AND METHODS

Reagents and Buffers. Unlabeled ribonucleoside triphosphates (NTPs) were purchased from P-L Biochemicals. [α-^{32}P]CTP (specific activity, 3000 Ci/mmol) was obtained from NEN. 3′-Deoxyribonucleoside triphosphates (dNTPs) were obtained from Boehringer Mannheim. ApU was from Sigma. DNA oligomers for PCR amplification were synthesized by Genosys Biotechnologies, Inc., as was the 42-bp insert for the construction of NInt′ template. Wild-type RNA polymerase was purchased from Epicenter Technologies. Rho factor was purified according to the procedure of Mott et al. (*34*) and generously supplied by Dr. K. Walstrom of our laboratory. Chemicals for buffers and gel electrophoresis (including acrylamide, bisacrylamide, TEMED, and ammonium persulfate) were all of analytical reagent or gel electrophoresis grade. The running buffer used in our gel electrophoresis experiments was called 1X-KBET and contained 50 mM Tris-HCl (pH 8.1), 50 mM boric acid, and 0.78 mM EDTA.

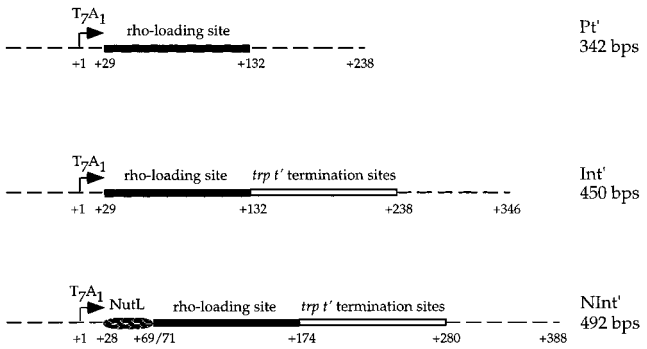

FIGURE 1: DNA templates containing the rho-dependent *trp t′* terminator used in this study. Filled and hollow bars represent DNA from the *E. coli trp t′* terminator, while broken lines denote DNA from carrier vector ptR2-5. Numbers on the right correspond to the total lengths of the DNA fragments, while numbers below the templates indicate the lengths of the transcripts to that point. The template positions of the T7A1 promoter, the *trp t′* rho loading site defined by Galloway and Platt (*30*, *31*), the DNA from the *trp* operon containing the *trp t′* rho-dependent termination sites, and the *NutL* element are all indicated. Template Pt′ carries the 104-bp rho loading site sequence immediately downstream of the T7A1 promoter, while template Int′ contains the intact *trp t′* terminator at the corresponding position. Template NInt′ differs from Int′ only by a 42-bp insertion containing the *NutL* element, which is placed upstream of the intact *trp t′* terminator sequence.

DNA Templates. The three different DNA templates used in this study are shown schematically in Figure 1. They were all made as double-stranded PCR amplification products from corresponding template plasmids. The template plasmid (pPt′) for transcription template Pt′ was constructed by inserting the 104-bp[2] *trp t′* rho loading site at the *Xma*I site just downstream of the T7A1 promoter in the previously described ptR2-5 plasmid (*39*). The template plasmid (pInt′) for transcription template Int′ was constructed by inserting the 218 bps of the *E. coli trp* operon that contains the rho-dependent *trp t′* terminator at the *Xma*I site just downstream of the T7A1 promoter in the ptR2-5 plasmid. The template plasmid (pNInt′) for transcription template NInt′ was constructed by insertion of a 42-bp fragment containing the phage *λnutL* sequence at the *Eco*RI site generated at the *Xma*I site downstream of the T7A1 promoter of pInt′. The 104-bp *trp t′* rho loading site and the 218-bp *trp t′* rho-dependent terminator sequence were isolated from plasmids pSP65t′ and pGEM1ΔMBt′, respectively (also generous gifts from the Platt laboratory), after digestion with *Eco*RI and *Pst*I. The sequences of all these template constructs were verified by DNA sequence analysis.

Rho-Dependent Transcription Termination Assays. Transcription reactions were carried out under standard reaction conditions [20 mM Tris-HCl (pH 7.9), 50 mM KCl, 5 mM $MgCl_2$, 1 mM β-ME] with 1 mM concentrations of each NTP at 37 °C, if not otherwise specified. Each reaction contained 5 nM DNA template, 5 nM RNA polymerase, and 20 nM rho hexamer in a final reaction volume of 10 μL. Transcription reactions were performed in two steps. First, the DNA template and RNA polymerase were incubated at 37 °C for 10 min, followed by the addition of 100 μM ApU, 50 μM ATP, 50 μM GTP, 50 μM CTP, and 2.5 μCi of [α-^{32}P]CTP. The reactions were then further incubated at 37 °C for 3 min, resulting in the formation of labeled elongation complexes stalled at position +25 (numbering from +1 as the transcription start site), since this is the first position on all our templates at which UTP is the next required nucleotide (see Figure 2). We note that these RNA chains are all radioactively labeled in the first 25 positions of the transcript.

In the second step of the assay a mixture containing a final 10 μg/mL concentration of rifampicin, the desired concentrations of all four NTP substrates, and rho and other proteins (or protein storage buffer) were added, and the reactions were further incubated at 37 °C for 5 min before transcription was "quenched" by the addition of a "stop" buffer reagent to final component concentrations of 25 mM EDTA, 1X KBET, 40% formamide, 0.05% bromophenol blue, and 0.05% xylene cyanol. Labeled RNA bands were then separated by size using polyacrylamide gel electrophoresis on 5% denaturing gels containing 8 M urea. Dried gels were scanned on a Storm Model 860 (Molecular Dynamics) radioactivity scanner, and the intensity distributions were analyzed using the ImageQuant Radioactivity Analysis Program (Molecular Dynamics).

Since the radioactive CTP used in the first step of the reaction was diluted more than 10000-fold in the second step under our standard reaction conditions, incorporation of the free radioactivity in the second step was negligible. As a consequence the RNA chains were not labeled at positions beyond +25, and thus the radioactivity at any given band position is a direct measure of the number of transcripts released at that point and is independent of transcript length.

Calculation of Rho-Dependent Termination Efficiency for the Overall Entire Terminator (TE_ρ) and for Individual Template Positions (Te_ρ). The *trp t′* terminator and its variants span significant portions of the templates that we have examined (Figure 2). To calculate the overall rho-dependent termination efficiency for a given terminator, the ImageQuant (Molecular Dynamics) software was used to draw "grid boxes" around the rho-dependent termination zone and the runoff transcript zone for reactions carried out in either the presence or the absence of rho, and the radioactivity contained in each of these zones was determined.

The overall rho-dependent termination efficiency for a given terminator sequence was calculated in two steps. First the background termination efficiency, TE_b, was measured in lanes containing the products of the transcription reaction run in the absence of rho. This parameter was determined by measuring the total apparent radioactivity appearing within the rho-dependent termination zone of the template, and dividing the value obtained by the sum of the same total radioactivity plus that measured at the runoff position. The reaction was then run in the presence of rho to obtain the overall total termination efficiency, TE_t, which includes both the background and the overall rho-dependent termination efficiency, TE_ρ.[3] Finally TE_ρ was calculated as

$$TE_\rho = (TE_t - TE_b)/(1 - TE_b) \quad (1)$$

[2] The 104 bp *trp t′* rho "loading site" used here differs from the original 105 bp site defined by Galloway and Platt (*30*, *31*) only in the lack of an rA residue at the very 3′ end of the former. The two sites have been shown to be functionally equivalent by the Platt laboratory (F. Zalatan, personal communication).

[3] Note that overall terminator efficiencies are designated TE, while termination efficiencies within individual grid boxes and at individual template positions are designated Te.

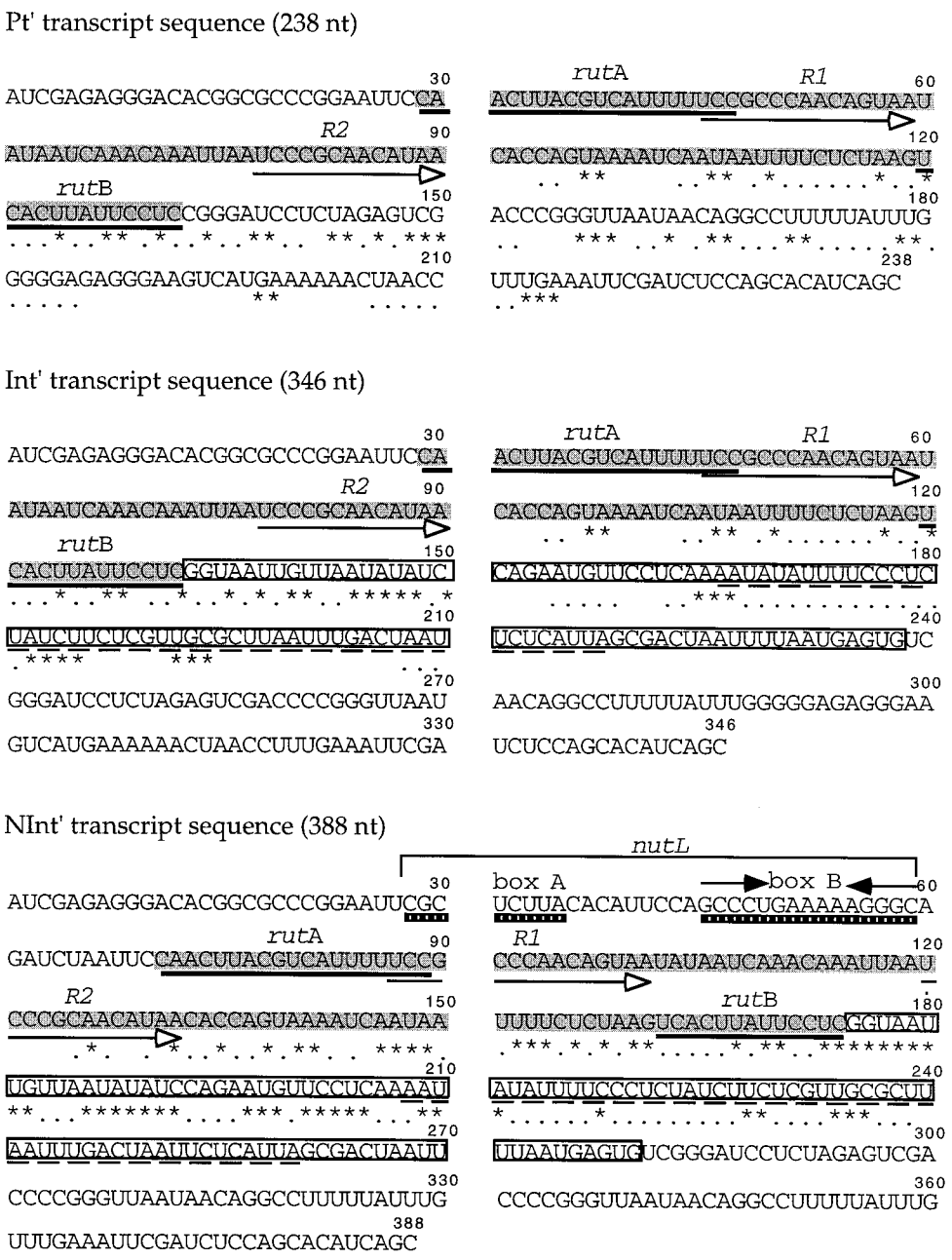

FIGURE 2: Transcript sequences of the *trp t′* terminator variants. Positions are numbered relative to the start point of transcription (+1). The *trp t′* rho loading sites (*30*, *31*) are shaded, and the sequence from the *E. coli trp* operon containing the rho-dependent termination sites are boxed. The *rutA* and *rutB* elements are underlined by thick lines, and the repetitive *R1* and *R2* elements are underlined by thin hollow arrows. The *NutL* element is indicated by a bracket above the sequence, and the λ boxA and boxB sequences are underlined by mosaic bars. The dyad sequences of boxB are shown by thick filled arrows facing one another above the sequence. Rho-dependent termination sites at the *trp t′* intact terminator mapped previously (*29*, *32*) are underlined with broken lines along the transcripts of templates Int′ and NInt′. Rho-dependent termination positions that we have mapped on each template (Figure 4) are indicated by black dots or stars below the sequences. These positions have been qualitatively designated as weak (dots) or strong (stars) termination positions on the basis of the relative intensities of the corresponding gel bands. We note that the "strengths" of individual termination positions defined in this way do not necessarily correlate with the value of the rho-dependent termination efficiency parameter (Te_ρ) at the corresponding position, since Te_ρ is defined as the number of elongation complexes that terminate at a given position divided by the number that reach that position or beyond on the template.

To calculate the fraction of the overall rho-dependent termination that occurs at individual gel band positions along the template, the rho-dependent termination region was divided into many small areas using the grid function of the ImageQuant program, and the radioactivity inside each small area was determined. The radioactivity within the runoff transcript region was determined in a single box. The termination efficiency for a given template position was then calculated in four steps, as shown in the right panel of Figure 3A. In step 1, the radioactivity inside each small grid box was divided by the total radioactivity contained in the entire gel lane above it, which is the sum of the radioactivity in the defined grid box, all the defined grid boxes above it in the lane, and the runoff transcript region. These values represent the background termination efficiency for an individual grid box (Te_b) for reactions run in the absence of rho and the total termination efficiency (Te_t), including both background and rho-dependent termination (Te), for an

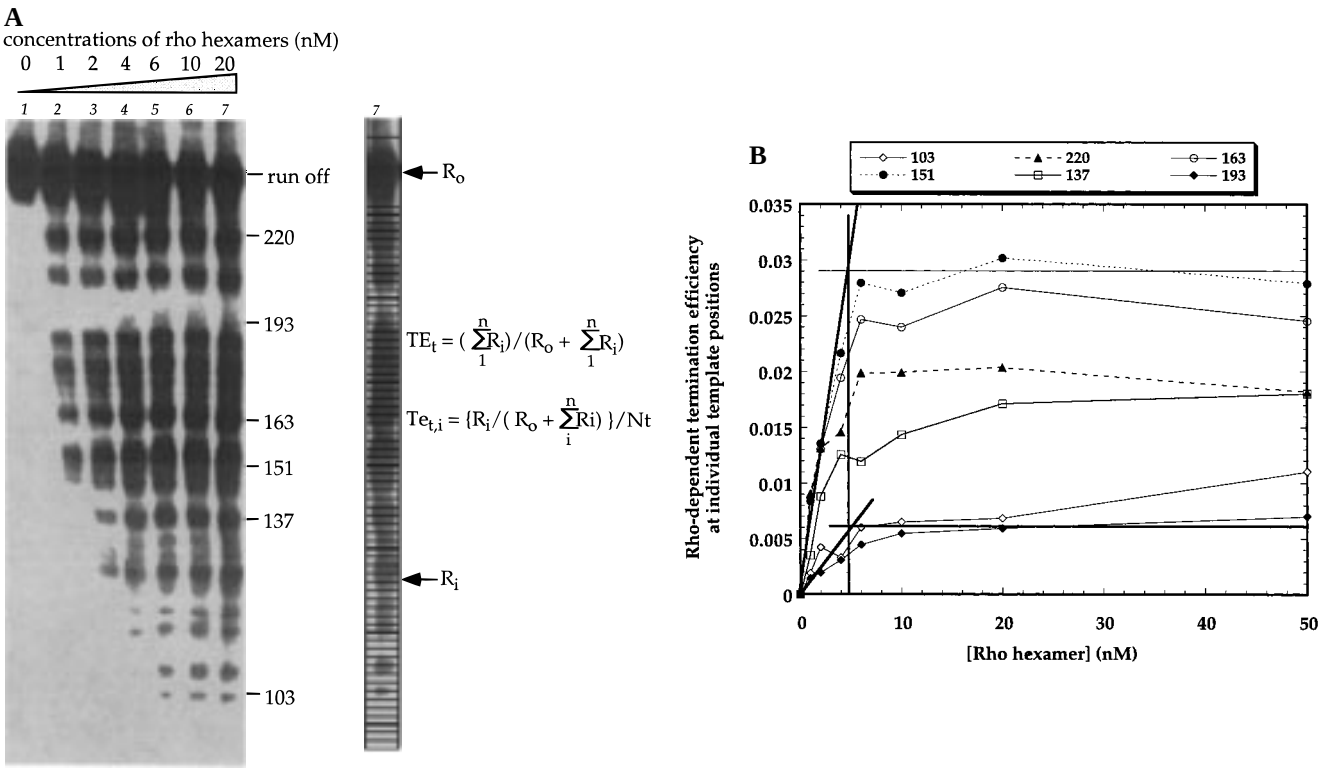

FIGURE 3: A single rho hexamer binds stoichiometrically and functions processively. (A) Rho-dependent termination as a function of rho concentration. Transcription reactions were performed as described in Materials and Methods in low salt (50 mM KCl) buffer and in the presence of 5 nM transcription complex (Pt′ DNA template), 1 mM of each NTP, and increasing concentrations of rho. Concentrations of rho hexamers in lanes 1−7 in the left panel are 0, 1, 2, 4, 6, 10, and 20 nM, respectively. Bands whose termination efficiencies are analyzed as a function of rho hexamer concentration in Figure 3B are marked along the right margin of the figure. Calculation of total overall termination efficiency (TE_t) and termination efficiencies at individual template positions (Te_t) are illustrated for lane 7 in the right panel. (B) Plots of Te_ρ as a function of rho hexamer concentration at various template positions. Data from Figure 3A. Calculations were made for bands located at template positions +103 (hollow diamonds), +137 (hollow squares), +151 (filled circles), +163 (hollow circles), +193 (filled diamonds), and +220 (filled triangles). Linear extrapolations of data sets +151 and +193 are shown explicitly (see text).

individual grid box for the same reaction carried out in the presence of rho. In step 2, rho-dependent termination efficiencies (Te) for each individual grid box were calculated as the difference between Te_t and Te_b as defined above, divided by the difference between unity and Te_b. In step 3, the number of transcript ends (Nt) in each grid area was calculated using RNA ladders as calibration markers. The logarithm of the length (in nts) of each RNA transcript in the RNA ladder was plotted as a function of pixel distance from top of the gel, and a straight line was fit to the data. On the basis of the equation for the resulting straight line, Nt was calculated as the difference in the transcript length that corresponds to the top and bottom of the grid box. Finally in step 4 the rho-dependent termination efficiency for each individual position along the template, Te_ρ,[3] was calculated by dividing the rho-dependent termination efficiency within the grid box (Te) by the number of transcript ends (Nt) within that grid box.

RESULTS

Template Design. Figure 1 shows the three variants of the *trp t′* terminator that were constructed and used in this study. Template Int′ encodes the intact *trp t′* rho-dependent terminator downstream of the strong T7A1 promoter and serves as the "standard" template. The Pt′ template differs from Int′ only in that the sequences that correspond to the natural rho-dependent *trp t′* termination sites have been deleted and replaced with foreign plasmid DNA, although the *trp t′* rho loading site of Int′ (as defined in ref *30*) was left intact. Template NInt′ differs from Int′ only in that it carries a 42-bp insert located upstream of the *trp t′* rho loading site, which encodes (in part) a stable RNA stem-loop hairpin structure called boxB.[4]

The elements of each template that are important in this study are illustrated in Figure 1. The RNA sequences of the runoff transcripts produced from these templates are shown in Figure 2. Also shown are the rho-dependent termination endpoints that have been mapped in this study, the termination endpoints mapped by Wu et al. (*29*) and by Zalatan et al. (*32*), the *rut*A, *rut*B, *R1*, and *R2* elements within the *trp t′* rho "loading site" that have been proposed by Zalatan et al. (*32*) to be important in rho-dependent termination within the *trp t′* sequence, and the *nutL* element containing the boxB (and boxA) sequences.

Single Rho Hexamers Bind Stoichiometrically and Function Processively in Rho-Dependent Transcript Termination. Our standard transcription assays were conducted at 37 °C in a reaction volume of 10 μL containing 5 nM DNA template and 5 nM RNA polymerase in the presence of 1 mM concentrations of each NTP, unless otherwise specified. Transcript elongation reactions were initiated from stable

[4] BoxB is the portion of the *nut* site that interacts specifically (as an RNA stem-loop hairpin) with phage λ-encoded N protein in N-dependent antitermination (e.g., see ref *47*). Here this sequence serves simply as a well-defined element of stable RNA secondary structure.

transcription complexes that had been stalled at template position +25 by omitting the next NTP required at that position (see Materials and Methods) and were run in buffer containing 20 mM Tris-HCl (pH 7.9), 50 mM KCl, 5 mM $MgCl_2$, and 1 mM β-ME. Rifampicin was also present in the reaction to prevent transcript reinitiation. Under these conditions rho induces efficient transcript termination on all of the templates used in this study.

Figure 3A shows the development of rho-dependent termination on template Pt′ as a function of the concentration of rho hexamers added. No measurable termination at template positions prior to runoff is seen in the absence of rho (lane 1). As the concentration of rho is increased, rho-dependent termination bands appear at a large number of defined template positions. We note that all of the (measurable) individual termination bands within the termination zone become progressively more intense as the concentration of rho is increased (lanes 2−4), that this increase in termination efficiency (both overall within the terminator zone and at individual bands) increases approximately linearly with increasing rho concentration, and that this increase appears (at most positions) to reach a plateau value at rho hexamer concentrations exceeding 5 nM (lanes 5−7). We used the procedures described in Materials and Methods to calculate the rho-dependent termination efficiency (Te_ρ) for several bands (marked in Figure 3A) along the template, as shown in Figure 3B.

Figure 3B shows that straight lines passed through the initial data points for representative bands from Figure 3A intersect with the plateau level of rho-dependent transcript termination for those bands at a total rho hexamer concentration of ∼5 nM. Furthermore the maximum (plateau) values of Te_ρ for each band are reached when the concentrations of rho hexamers and DNA and active transcription complexes become equal at ∼5 nM, and the Te_ρ values for individual gel bands at various template positions within the termination zone remain approximately constant at higher rho concentrations. This indicates, as also shown in studies of the helicase activity of rho using the same transcripts (*10, 36*), that the rho hexamers added are fully active in termination, and also that the transcription complexes that have been extended are also fully active and that rho hexamers interact approximately stoichiometrically with the functional transcription complexes under these reaction conditions. The latter conclusion is also consistent with direct-binding measurements (*36*) that show the binding constant (K_d) for rho to the loading site of these transcripts in 50 mM KCl is ∼1 nM.

These results can be further understood in the context of rho helicase studies (*10, 36*), which have shown that rho hexamers continue to bind to the RNA transcript after RNA−DNA strand separation under the salt concentrations used in this study (50 mM KCl). Hence rho cannot be recycled under these reaction conditions (i.e., at substoichiometric concentrations of rho) to rebind to unreacted transcription complexes and bring about further rho-dependent termination. Our results are thus consistent with the following model for rho-dependent termination. We posit that (i) a single rho hexamer binds tightly to the rho loading site of the nascent RNA of each transcription complex; (ii) rho "catches up with" the transcription complexes at a number of positions along the transcript; and (iii) single rho hexamers must translocate essentially processively along the nascent transcript under these conditions to bring about efficient rho-dependent termination at a large number of template positions. A 20 nM concentration of rho hexamers was used in the remainder of the termination assays described in this study to ensure that rho was present in excess.

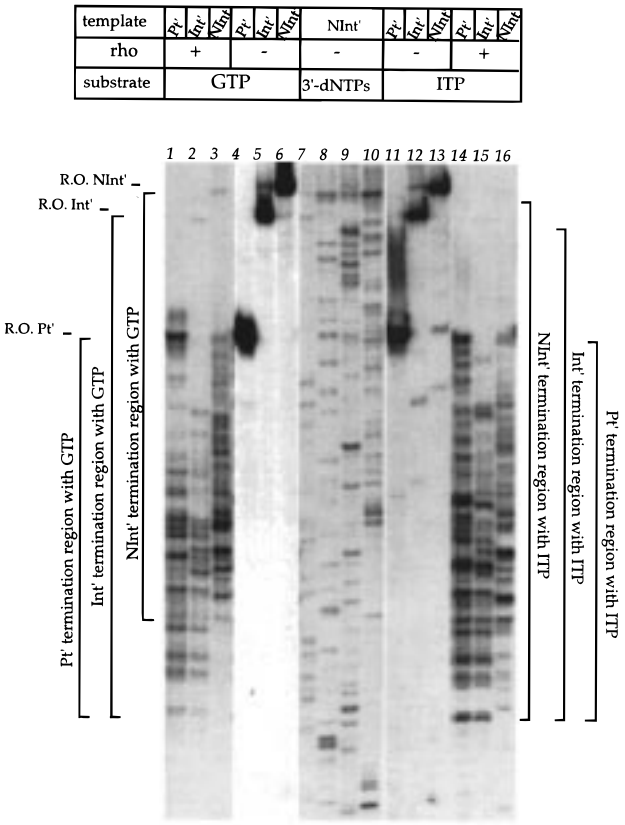

FIGURE 4: Mapping of rho-dependent transcription termination positions on all *trp t′* templates for transcripts containing either rG or rI residues. Reactions were carried out under our standard transcription conditions (see Materials and Methods) in the presence of 5 nM transcription complex, and 0 or 20 nM rho hexamers. Transcription reactions on different templates after rG incorporation are in lanes 1−6, reactions with rho present are in lanes 1−3, and reactions without rho are in lanes 4−6. Transcription reactions on the different templates after rI incorporation are in lanes 11−16. Rho is present in lanes 14−16 and absent in lanes 11−13. Radioactive bands that correspond to the runoff transcript of each template are marked in the left margin. Rho-dependent termination regions for each template for transcripts containing rG are indicated by brackets in the left margin, and those containing rI are marked in the right margin. RNA ladders prepared by 3′-dNTP incorporation on the NInt′ template were run in parallel in lanes 7−10, and serve as transcript size markers.

Mapping of Rho-Dependent Termination Positions within the trp t′ Terminator on various Templates. The results presented in Figure 3A have shown that the zone over which rho-dependent termination extends is large, and that the intensities of bands at various template positions within this zone are heterogeneous. These facts permit us to map and characterize patterns of rho-dependent transcript termination (RNA release) over a wide range of template positions as a function of reaction conditions. Figure 4 shows some of these results for each of the DNA templates. In all these experiments, RNA sequencing ladders, generated by including chain-terminating nucleotides (3′-dNTPs) in the transcription mix in the absence of rho, have been run in parallel with our rho-dependent termination assays to serve as standards of transcript length (lanes 7−10).

In lanes 1−3 of Figure 4 (as well as in lanes 14−16) we show that the zone of effective rho-dependent termination for the *trp t′* terminator extends for more than 100 nts along the templates that we have examined. This heterogeneity of termination positions within the *trp t′* terminator zone is in marked contrast to the behavior of intrinsic terminators (e.g., the *tR2* terminator, see ref *25*), for which significant termination occurs only at two or three neighboring template positions per terminator. This behavior of the rho-dependent *trp t′* terminator also contrasts with observations on other well-characterized rho-dependent terminators within which rho-dependent termination also occurs at fewer template positions (for example, the *tR1* terminator of phage λ consists of five discrete clusters of sharply defined termination positions; see refs *40*, *41*).

Figure 4 shows that transcription in the absence of rho is very processive on all these templates under the reaction conditions used, and that most of the elongation complexes formed are converted to runoff transcripts (lanes 4−6, as well as lanes 11−13). This finding, together with examination of the template sequences (Figure 2), shows that these templates carry no intrinsic terminators. In addition, even though rho causes heterogeneous termination along each template (lanes 1−3), the patterns of individual rho-dependent termination bands are discrete and can easily be differentiated from patterns obtained with other templates. Figure 4 also shows that rho-dependent transcript termination begins at essentially the same position on the Pt′ and the Int′ templates (lanes 1 and 2), while it begins considerably further downstream on template NInt′ (lane 3). A qualitative summary of the positions and intensities of all the rho-dependent termination bands seen with these templates is included in Figure 2, where small dots below individual sequence positions correspond to positions of apparent weak termination and stars correspond to apparent strong termination positions.

The overall efficiency of rho-dependent termination (TE_ρ), defined as the fraction of elongation complexes within the whole population that terminate before reaching the end of the template in the presence of rho (see Materials and Methods), is close to unity for those templates that contain the entire *trp t′* terminator (e.g., templates Int′ and NInt′, which include both the rho loading site of *trp t′* and the *trp t′* termination zone). With these templates we have obtained TE_ρ values of ∼0.95 for template Int′ and ∼0.98 for template NInt′. This means that rho is essentially fully efficient in bringing about transcript termination when it catches up with an individual elongation complex under the experimental conditions of this study, and that the design of the *trp t′* terminator is such that virtually all of the transcription complexes are "caught" by rho within the terminator zone, even though the actual positions at which rho-dependent termination occurs are spread widely along the DNA template.

Furthermore we have shown that TE_ρ is ∼0.75 even for template Pt′, which contains the rho loading site of the *trp t′* terminator, but in which the actual *trp t′* termination zone has been replaced by a foreign plasmid DNA sequence that contains no natural rho-dependent terminators. Generalizing from this result, we suggest, as was also concluded by Richardson and Richardson (*42*) on the basis of a similar experiment, that the primary determinant for rho-dependent termination is a functional rho loading site, and that if such a loading site is present, sufficient pausing is likely to occur within an arbitrary DNA sequence of about 100 nts to lead to extensive rho-dependent termination. These results, which are also consistent with those of Walstrom et al. (*10*, *36*) in which rho helicase activity was assayed on essentially the same transcripts and under comparable buffer conditions, suggest that rho hexamers move processively along the nascent transcript from the rho loading site and that they can efficiently terminate any transcription complex within the termination zone under these reaction conditions.

To investigate these outcomes more thoroughly, we have quantified the efficiencies of rho-dependent termination as a function of template position across the *trp t′* terminator within each lane of Figure 4. In Figure 5A−D, we plot the measured rho-dependent termination efficiencies at individual template positions (Te_ρ) to obtain a pattern of rho-dependent termination efficiency for each template. Such quantitative analyses of the rho-dependent termination reaction on each template are independent of arbitrary factors such as gel loading, and thus can be directly compared to reveal features of the rho-dependent termination process.

Patterns of Rho-Dependent RNA Release as a Function of Template Position. In Figure 5A we compare patterns of rho-dependent termination efficiency (Te_ρ) as a function of template position between positions +75 and +300 (or the end of the template for Pt′) for all three templates that we have studied. Measurements near the 5′ end of the template show that no rho-dependent termination is observed on either template Pt′ or template Int′ at positions upstream of +97. In contrast, rho-dependent termination on template NInt′ does not begin until position +123. Downstream of these positions, Figure 5A shows that rho-dependent termination occurs over a wide range of dispersed sites on all three templates.

Closer examination of Figure 5A also suggests that, within the termination zone on each template, less rho-dependent termination is generally seen in the 5′ upstream region (upstream of position +103 on templates Pt′ and Int′ and upstream of position +130 on NInt′) and in the 3′ downstream region near the end of the template (beyond position +180 on template Pt′, +240 on Int′, and +280 on NInt′), and that the bulk of rho-dependent termination occurs mostly between positions +130 and +160 on template Pt′, between positions +130 and +200 on template Int′, and between positions +135 and +250 on template NInt′. One common feature of the rho-dependent RNA release patterns for all these templates is that rho-dependent termination appears to be most efficient around template position +150. We have compared the sequences of the templates and detected no homology in this vicinity between any of the three templates that we have studied (Figure 2). This finding is consistent with earlier results with the rho-dependent *tR1* terminator, which also showed that individual clusters of high termination efficiency within this terminator displayed little or no sequence homology (*41*). We suggest that such overall length-dependent periodicities relate more to the transcript length dependence of the wrapping of the RNA around the rho hexamer (see ref *38*) than to the effects of local RNA sequence. These results are also compatible with the length-dependent periodicities of rho ATPase activation by poly-

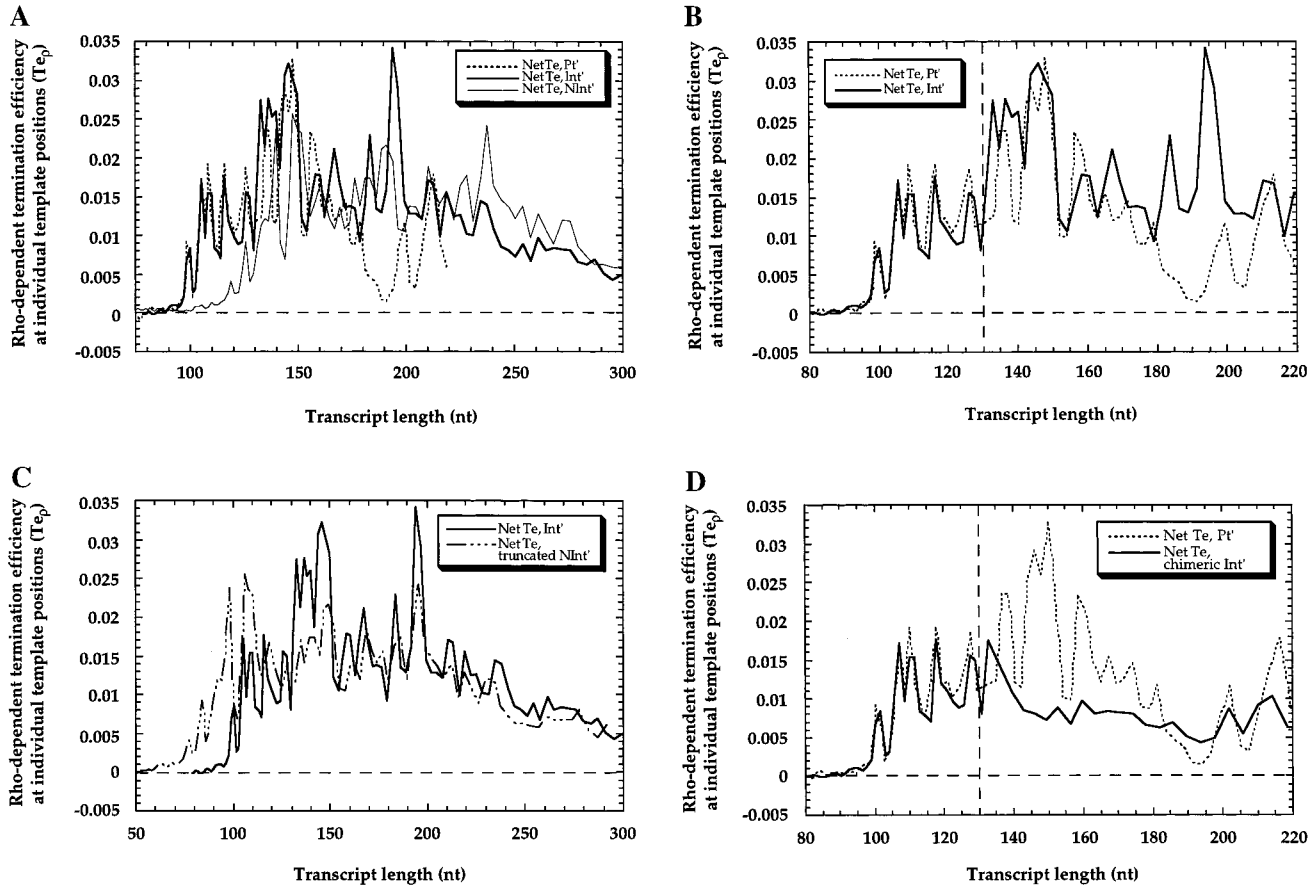

FIGURE 5: Rho-dependent RNA release patterns as a function of template position. Typical gels of transcription reactions run with GTP, as shown in Figure 4, lanes 1−6, have been quantified and rho-dependent termination efficiencies at individual sites calculated (see Materials and Methods). The broken horizontal line is the baseline representing 0 rho-dependent termination efficiency. (A) Comparison of rho-dependent RNA release patterns for all the templates. The dotted line corresponds to the release pattern for template Pt′, the dark solid line plots the release pattern for template Int′, and the faint solid line plots the release pattern for template NInt′. It is evident that template zones containing rho-dependent termination positions are broad and heterogeneous on all the templates, and that termination actually begins within the previously defined (*30*, *31*) rho loading site that ends at position +132 for templates Pt′ and Int′ and at position +174 for template NInt′. (B) Rho-dependent termination efficiencies at individual template positions are dependent on local template sequence. The dotted line represents the release pattern for template Pt′, and the solid line represents the pattern for template Int′. The broken vertical line marks the position at which the sequences of the two templates start to differ. (C) Individual termination efficiencies are dependent on local sequence but are also affected by rho-loading. The solid line represents the release pattern for template Int′, and the dashed line represents the pattern for truncated template NInt′, which has been "reduced in length" by 42 nts by calculation (see text). The rho-dependent termination efficiency patterns of the Int′ and NInt′ templates have been aligned with the actual sequence, with the template positions "normalized" to those of the Int′ template. (D) The same template sequence, placed 106 nt farther downstream from the rho loading site, supports much less efficient termination**.** The dotted line represents the release pattern obtained with template Pt′, and the solid line represents the pattern obtained with a "chimeric" Int′ template, with the pattern corresponding to the sequence of Int′ between positions +132 and +238 removed. The rho-dependent termination efficiencies at individual template positions shared by Pt′ and Int′ have been aligned according to the actual sequence. The numbering of the transcript positions shown is based on the Pt′ template. The broken vertical line marks the position at which the template sequences shared by Pt′ and Int′ are "artificially" joined to create the chimeric Int′ template.

(rC) that have been reported by McSwiggen (*43*). Examination of these quantitative RNA release patterns leads to the following conclusions.

(i) Neither the Entire Rho Loading Site Nor the rutB Sequence Is Required for Rho-Dependent Termination. It has been suggested, on the basis of deletion experiments, that the *rut* sequences within *trp t′* may serve as important sequence elements in activating rho-dependent termination (*32*). We note in Figure 5A that substantial rho-dependent termination occurs with all the templates we have used before transcription has reached the end of the 104-nt rho loading site, even though the downstream end of the loading site carries the *rut*B sequence element. The rho loading site [as defined by Galloway and Platt (*30*, *31*)] ends at position +132 on both templates Pt′ and Int′ (Figure 2), but rho-dependent termination begins at position +97 on these templates (Figure 5A), which is 35 nts upstream of the position at which synthesis of the loading site (and the *rut*B element) is complete.

The same observation was made using the NInt′ template, in which the 42-bp insert positioned upstream of the rho loading site represents the only difference between this template and the Int′ template. This insert shifts the first termination position on NInt′ downstream by 26 nts relative to Int′ (see Figure 5A). On the NInt′ template the rho loading site ends at position +174 (Figure 2), but termination starts at position +123, which here falls 51 nts upstream of the end of the loading site and of the *rut*B element. In fact, the most efficient termination positions on the NInt′ template fall in the vicinity of positions +140 to +150, which are clearly located in the middle of the loading site and well upstream of the *rut*B element.

Since the RNA-dependent ATPase activity of rho is known to be essential for rho-dependent termination, rho must have been loaded onto the RNA before the transcription complex had reached position +97 on templates Pt′ and Int′, and position +123 on NInt′, where rho-dependent termination begins to be observed (Figure 5A). These findings are inconsistent with the previous definition of the rho loading site of this terminator, and suggest that completion of neither the entire *trp t′* rho loading site nor the *rut*B sequence (nor perhaps of other putative rho-activating sequences as well) is required to turn on fully efficient rho-dependent termination under the reaction conditions used here.

The *trp t′* rho loading site was originally defined under conditions of higher salt (150 mM KCl) and lower NTP substrate concentrations (*30, 31*). We show in the companion paper (*38*) that under these conditions the effectiveness of rho loading and the processivity of rho translocation are both reduced, and that the RNA sequence requirements for rho-dependent termination do indeed agree with the original definition of the rho loading site. Thus the sequence requirements that define a rho loading site are clearly condition-dependent.

(ii) Rho-Dependent Termination Requires a Minimum Transcript Length of ~97 nts. Earlier observations have suggested that unstructured RNA sequences are required to serve as a rho loading site and also that the minimum length of unstructured nascent transcript that will support rho-dependent termination on a number of templates is 85−105 nts (*5*−*7, 44, 45*). Figure 5A shows that rho-dependent termination on templates Pt′ and Int′ begins at position +97, well before completion of synthesis of the *trp t′* rho loading site defined by Galloway and Platt (*30, 31*).

To explain this observation further we consider the possibility that the 28-nt cytidine-rich transcript of the T7A1 promoter (the *trp* promoter followed by the *trp* leader sequence had been used in previous studies of the *trp t′* terminator; *30, 31*) might serve as part of an extended rho loading site on the templates used in this study. This possibility was tested by scanning the first 97 nts of the transcripts from the Pt′ and the Int′ templates, and the first 123 nts of the transcript from template NInt′, with the Mulfold RNA Secondary Structure Analysis Program (*46*). We found that the first 97 nts of the Pt′ and Int′ transcripts (including the portion of the T7A1 promoter that is transcribed) were predicted to be essentially free of stable RNA secondary structures, while the 15-nt boxB hairpin sequence was defined as the only stable RNA structure within the first 123 nts of the NInt′ transcript. On the other hand the RNA transcribed from the *trp* promoter and the *trp* leader sequence is predicted to be full of stable RNA secondary structure.

The 26-nt downstream shift of the first termination site observed for transcription on the NInt′ template indicates that the transcript generated by a 42-bp insert into the template cannot be completely utilized by rho, since then rho-dependent termination would start at template position +97 with the NInt′ template as well, nor is it completely ignored by rho since termination would then begin at position +139 (i.e., 97 + 42 = 139). This intermediate result suggests that only a part (about 16 nts) of the NInt′ template insert can be used by rho to activate rho-dependent termination.

(iii) Rho-Dependent Termination Efficiency Is Dependent on Template Sequence. Templates Pt′ and Int′ differ in sequence from position +132 on, with plasmid DNA sequences following this position on template Pt′ and the natural *trp t′* terminator sequences following on template Int′ (Figure 1). Figure 5B shows that the patterns of rho-dependent termination efficiency at individual template positions overlap well on templates Pt′ and Int′ at positions upstream of +132, but start to deviate significantly thereafter, suggesting that the fine structure of these rho-dependent RNA release patterns may depend on template sequence at or near the 3′ ends of the released transcripts. We note that the magnitude of the measured patterns of rho-dependent termination over the 50 nts downstream of position +132 appears similar, even though the DNA (and RNA) sequences in this region of the templates are totally different, suggesting again that rho-dependent termination efficiency is dependent on sequences located considerably upstream of the actual positions at which termination occurs.

These results suggest that the primary sequence determinants that are responsible for these pattern similarities fall at or near the transcript ends, while secondary determinants can reflect sequence similarities that extend as far as 50 nts or more upstream of the 3′ ends of the terminated transcripts. We have analyzed the RNA release pattern for another template that differs from Pt′ only in a 9-bp sequence in the middle of the template (this difference does not result in any significant formation of RNA secondary structure) and found that the rho-dependent RNA release patterns obtained for the two templates overlap very well except at the template positions of the sequence difference itself (data not shown); this is consistent with a local sequence effect on rho-dependent termination efficiency.

(iv) The Absolute Magnitudes of the Rho-Dependent RNA Release Patterns Depend on the Structure and Sequence of the Transcript Upstream of the Actual Termination Zone. In Figure 5C, we compare the RNA release pattern obtained with template Int′ with that obtained with a "truncated" template NInt′ from which the template positions corresponding to the 42-bp insert have been "deleted" by calculation (i.e., the NInt′ transcript pattern has been shifted 42 bps to the left in Figure 5C by omitting the NInt′ pattern of Figure 5A between positions +28 and +69). As a consequence the template positions of the NInt′ pattern are aligned with the corresponding positions along the Int′ template (see Figure 1).

We have found that, except for the initial termination within the rho loading site (upstream of position +132 on template Int′), the RNA release patterns within the natural *trp t′* termination region (between positions +133 and +238 on Int′) are similar on both templates, again reflecting the dominant effect of local sequence at or near the potential 3′ ends of the transcripts on the extent of termination. However, we have also observed that the absolute values of the rho-dependent termination efficiencies are lower at corresponding positions along the NInt′ template than along the same sequences of the Int′ template. We conclude that while the overall patterns of these rho-dependent termination patterns are strongly dependent on the local template sequence, the absolute magnitudes of the patterns may be perturbed by rho loading events.

Since the only structural differences between NInt′ and Int′ at equivalent template positions as plotted in Figure 5C is the 42-bp insert containing the boxB RNA hairpin, the quantitative differences in the heights of the similarly shaped RNA release patterns that extend about 70 bps downstream of position +132 may reflect that rho loading is more effective (i.e., for template Int′) when the rho hexamer does not have to contend with elements of secondary structure (such as boxB) located within (or downstream of) the actual rho loading site. An alternate possibility is that the distance between the corresponding termination site and the actual rho loading site is shorter on Int′, so that more complexes are "caught" by rho at these individual positions than at the equivalent positions along the NInt′ template. These possibilities are examined elsewhere in quantitative terms (A. Q. Zhu, M. O'Neill, and P. H. von Hippel, manuscript in preparation).[5]

(v) Large Upstream Sequence Differences Can Totally Change Rho-Dependent RNA Release Patterns. In Figure 5D we have aligned the RNA release patterns for template Pt′ and a "chimeric" template Int′ by "leaving out" the natural rho-dependent termination positions of the *trp t′* terminator that fall between positions +132 and +238 of the Int′ template, thus permitting the alignment of the common downstream regions of the two templates (see Figure 1). The results show that the two patterns are closely similar up to position +132 (as discussed in (iii) above) and that beyond this point the patterns are almost totally dissimilar. Since the artifical "truncation" procedure that we have used places identical sequences at the 3′ ends of the templates beyond position +132, the results suggest that the RNA release patterns also strongly depend on the overall RNA sequence of the section of the transcript to which rho is actually bound when it is bringing about RNA release, or on the distance between the actual site of rho loading and the termination positions. Comparison of the two patterns beyond position +132 suggests that overall termination is much less efficient for the downstream positions of the Int′ template than for the equivalent positions on the Pt′ template.

Conclusions from the Analysis of RNA Release Patterns. In summary, our results appear to be consistent with the notion that the efficiency of rho-dependent termination in any region of the template depends on the sequence of the transcript near the putative 3′ end positions at which rho-dependent termination occurs, on the distance between the actual site of rho loading and the termination site, and on the overall sequence and RNA secondary structure content of the region of the transcript that lies upstream of this position. When the sequences in these regions are the same, the rho-dependent patterns of RNA release are also the same. Generalizing from the examples worked out in detail here, we argue that when short lengths of sequence upstream of the 3′ ends of the rho-terminated transcripts differ, or contain significant elements of secondary structure, the termination patterns at identical sequences will have the same shape but may differ in magnitude, with elements of strong secondary structure decreasing the magnitude of the RNA release observed at a given template position (see Figure 5C). When long elements of upstream sequence differ, as in Figure 5D, rho-dependent termination patterns within sequences that are identical at the 3′ ends may differ completely. Further interpretations of these observations, couched in terms of the structure and RNA interactions of the rho hexamer, are presented in Zhu and von Hippel (*38*) and elsewhere (A. Q. Zhu, M. O'Neill, and P. H. von Hippel, manuscript in preparation).

IMP Incorporation into the Nascent Transcript Moves the Start of RNA Release to Position +97 for the NInt′ Template. The above conclusions led us to ask whether the 26-nt distal shift of the first termination sites on the NInt′ template observed in Figure 5A is a consequence of the changed sequence of the intervening transcript segment, or whether it reflects interference of the secondary structure of the boxB RNA hairpin with proper binding of the rho hexamer to the transcript. To examine this question further, we substituted ITP for GTP in the transcription reaction, which results in the replacement of rG residues with rI residues in the nascent transcript. Since rI·rC bps are much "weaker" (with respect to thermal disruption) than rG·rC bps, this substitution largely eliminates stable secondary structure from the nascent transcript (see ref *12*). We then mapped the rho-dependent termination zone for each template after rI incorporation into the transcript (Figure 4, lanes 11−16) and compared the results with those obtained with the rG-containing transcripts (lanes 1−6).

Elongation in the absence of rho is very processive with either GTP (Figure 4, lanes 4−6) or ITP as a substrate (lanes 11−13). In addition, rho-dependent termination is much more efficient at all templates for transcripts containing rI residues (lanes 14−16) instead of rG residues (lanes 1−3). Plots of termination efficiency at individual template positions under these different conditions are not presented. However, we have observed that both the positions of the rho-dependent termination zones and the rho-dependent RNA release patterns are the same for templates Pt′ and Int′, while for template NInt′ the incorporation of rI residues shifts the start point of the termination zone from position +123 for rG-containing transcripts to position +97 for rI-containing transcripts. Thus the substitution of rI for rG residues in the transcript shifts the beginning of the rho-dependent termination zone to the *same* position for all three templates.

This result is consistent with the prediction of the Mulfold program that no stable RNA secondary structure is associated with the first 97 nts of transcripts made on the Pt′ and Int′ templates, because IMP incorporation does not shift the termination zone upstream on these templates. On the other hand the dramatic proximal shift along template NInt′ of the first termination position after rI residue incorporation strongly suggests that it is the disruption of the stable rG·rC pairing within the stem of the boxB RNA hairpin that is responsible for this shift of the terminator along the template. To be sure that this result is not due to a kinetic effect, we also measured the rate of elongation on the NInt′ template at the new termination sites between positions +97 and +123 with ITP as a substrate by the procedures described in the companion paper (*38*), and showed that the rate is comparable to that with GTP as a substrate in this template region

[5] We note that the these results cannot be ascribed to functionally heterogeneous populations of either rho or transcription complexes. RNA binding experiments (*36*) have shown that the rho population used in this study is homogeneous and fully active. The titration of transcription complexes with rho described in Figure 3A demonstrates that the transcription complexes formed in these studies are also functionally homogeneous and fully active.

(data not shown). The result is compatible with the sequence of this template between positions +97 and +123 (Figure 2) since this region codes for a transcript that contains only a single rG residue (at position +98) where rI residue substitution could possibly alter the rate of elongation. Thus it is very unlikely that the upstream shift of the termination zone at NInt′ is due to a slower elongation rate in this region in the presence of ITP. Furthermore, since NInt′ is the only template that showed an upstream shift of the rho-dependent termination zone after incorporation of rI, we can also conclude that this proximal shift of the rho-dependent termination zone does not reflect any general change in the properties of the transcription elongation complex as a consequence of the incorporation of rI residues into the transcript.

DISCUSSION

In this study we have approached the mechanism of action in transcript termination of *E. coli* transcription factor rho by means of a careful examination of the fine structure of the rho-dependent RNA release pattern along the *trp t′* terminator. The *trp t′* terminator differs from most rho-dependent terminators that have been carefully investigated in the past in that this terminator, defined as the sequence over which significant rho-dependent termination takes place, spans more than 100 bps along the template DNA. Normally this might be considered a disadvantage in a quantitative study of termination efficiency, but here it turns out to be an advantage in that we have been able to correlate various changes in template sequence and reaction conditions with changes in the fine structure of the RNA release pattern along the terminator.

RNA Release Patterns. These patterns (e.g., see Figure 5A−D) do not merely represent distributions of RNA band intensities along the template. Rather they are actual patterns of the rho-dependent termination efficiency at each template position (which we have termed Te_ρ; see Materials and Methods), since this parameter is corrected not only for any rho-independent termination that may occur at a given template position and for any rho-dependent termination that may have occurred upstream, but also for the logarithmic distribution of RNA transcripts of different length on the gel. Thus Te_ρ, which is a fraction less than unity, is defined as the number of RNA chains released at a given template position as a consequence of rho action, divided by the total number of transcription complexes that arrive at that position and either terminate there or continue downstream.

As a consequence, the Te_ρ parameter is independent of the fraction of nascent transcripts that have been released upstream, which is not the case if one simply plots RNA band intensity as a function of template position, and this permits us to make unbiased comparisons of alterations in rho-dependent termination efficiency as a function of changes in template sequence or reaction conditions in transcription assays. For comparison we have also defined a parameter called TE_ρ, which represents the overall rho-dependent termination efficiency across the entire terminator. This parameter is also a fraction and is defined as the number of RNA chains released as a consequence of rho action within the entire terminator, divided by the total number of transcription complexes that release RNA (due to rho action) anywhere along the terminator sequence plus those that reach the runoff position without having released their RNA chains. In this sense TE_ρ is a "lumped" parameter that defines the overall efficiency of a rho-dependent terminator sequence, whether confined to one or two template positions or spread across one hundred positions or more. We note that TE_ρ is *not* the sum of the Te_ρ values measured at the individual template positions within the terminator, since each of the latter parameters is, by definition, independent of the termination that has occurred before (for a more extensive discussion of this point, see ref *25*).

Overview of Rho-Dependent Termination with Templates Carrying Components of the trp t′ Terminator. We can summarize our present findings on the properties of rho-dependent terminators, couched in terms of our analysis of the *trp t′* terminator, as follows.

(i) Under the salt conditions used here (50 mM KCl + 5 mM $MgCl_2$), the overall efficiency (TE_ρ) of the rho-dependent *trp t′* terminator is close to unity, meaning that the overall terminator is totally efficient, even though transcript release is spread over more than one hundred individual template positions. The fraction of nascent transcripts released as a consequence of rho action at a given template position is Te_ρ, and this parameter varies from 0.03 to 0.001 or less within the *trp t′* terminator at the maximum rates of both the rho termination function and the elongation activity of the transcription complex.

(ii) The template sequence of the *trp t′* terminator itself contains two parts, consisting of ∼104 nts of unstructured RNA at the 5′ end of the nascent transcript where the rho hexamer binds and its RNA-dependent ATPase is activated, followed by a downstream portion of ∼120 bps of DNA over which rho-dependent transcript release actually occurs.

(iii) A single rho hexamer binds stoichiometrically to each rho loading site as it is synthesized, and then moves processively along the nascent transcript until it catches up with the elongating transcription complex and releases the newly formed transcript. We note that each template carries only a single transcription complex and makes only a single transcript. As a consequence, under these reaction conditions each rho hexamer releases a single transcript with an efficiency of unity, but the rho hexamers move in an unsynchronized fashion and the RNA release patterns represented by Figure 5A−D correspond to a weighted distribution of template positions at which the individual rho hexamers actually bring about transcript release.

(iv) A minimum of ∼97 nts of transcript must be synthesized before any rho-dependent termination can occur. This RNA forms the loading site for the rho hexamer (except for those RNA residues at the 3′ end of the transcript that are still transiently engaged as a part of the transcription complex) and must be essentially free of secondary structure to function efficiently. This is demonstrated by inserting a defined RNA hairpin (the boxB sequence of phage λ) into this loading site region of the template, which significantly increases the length of the transcript that must be synthesized before rho-dependent termination can begin. That this inhibition is due to the presence of stable RNA secondary structure in the nascent transcript is demonstrated by replacing rG residues within the transcript with rI residues that cannot engage in the formation of stable RNA secondary

structure. The length of transcript required before rho action can begin then reverts to ~97 nts.

(v) The efficiency with which rho-dependent termination can occur at a given template position (Te_ρ) within the zone of termination depends on the local sequence in the vicinity of the putative 3′ end of the corresponding transcript at that position. Characteristic RNA release patterns are formed under standard transcription conditions that reflect largely the sequence of the terminator within the termination zone. We assume that these local sequence effects reflect primarily features of the interaction of the local transcript and the template sequence with the components of the transcription complex, including how long the transcription complex remains at that position (i.e., pausing), the stability of the transcription complex, and the accessibility of the RNA−DNA hybrid within the transcription bubble to rho (see ref *38*; and A. Q. Zhu, M. O'Neill, and P. H. von Hippel, manuscript in preparation), although differences in the action of rho on transcription complexes in different conformational states may also be involved (A. Q. Zhu, M. Kashlev, and P. H. von Hippel, manuscript in preparation). Termination efficiency at a given template sequence decreases with increase in its distance from the actual site of rho loading (Figure 5C,D); this is discussed elsewhere (A. Q. Zhu, M. O'Neill, and P. H. von Hippel, manuscript in preparation) in the context of other findings.

(vi) The upstream limit of rho-dependent termination, and thus the position of the zone of opportunity for rho-dependent termination, depends on the synthesis of a length of RNA transcript sufficient to form an effective loading site for the rho hexamer. The amount of RNA that is required for this purpose can be increased, thus resulting in a distal shift of the zone of opportunity for rho-dependent termination, by introducing elements of RNA structure into the nascent transcript, either specifically by inserting a sequence that can form a structured RNA element, or nonspecifically by increasing the secondary structure of the transcript as a consequence of an increase in the concentrations of mono- or divalent cations in the reaction buffer (see ref *38*).

(vii) The structure and sequence requirements for the rho loading zone appear to be relatively simple, including only a lack of stable secondary structure over a fairly large binding site and perhaps a minimal requirement for rC residues. We have found no requirement for specific rho-activating sequences such as the postulated *rut* sites (see ref *37*). In fact not even synthesis of the whole *trp t′* rho loading site, which was initially defined as being 105 nts in length by Galloway and Platt (*30*, *31*), is required under the conditions examined in this paper, since the minimal transcript length needed for loading a single rho hexamer is appreciably less (see also ref *36*).

ACKNOWLEDGMENT

We are grateful to Terry Platt and his laboratory at the University of Rochester for the generous gift of plasmids pSP65t′ and pGEM1ΔMBt′, to Katherine Walstrom of this laboratory for providing rho protein, and to Marc Van Gilst and Feng Dong for many helpful discussions of techniques and results.

REFERENCES

1. Roberts, J. W. (1969) *Nature 20*, 1168−1174.
2. Bear, D. G., and Peabody, D. S. (1988) *Trends Biochem. Sci. 13*, 343−347.
3. Richardson, J. P. (1990) *Biochim. Biophys. Acta 1048*, 127−138.
4. Platt, T., and Richardson, J. P. (1992) in *Transcriptional Regulation* (McKnight, S. L., and Yamamoto, K. R., Eds.) pp 365−389, Cold Spring Harbor Laboratory Press, Cold Spring Harbor, New York.
5. Morgan, W. D., Bear, D. G., Litchman, B. L., and von Hippel, P. H. (1985) *Nucleic Acids Res. 13*, 3739−3754.
6. Bear, D. G., Hicks, P. S., Escudero, K. W., Andrews, C. L., McSwiggen, J. A., and von Hippel, P. H. (1988) *J. Mol. Biol. 199*, 623−635.
7. Hart, C. M., and Roberts, J. W. (1991) *J. Biol. Chem. 266*, 24140−24148.
8. Howard, B., and de Crombrugghe, B. (1976) *J. Biol. Chem. 251*, 2520−2524.
9. Brennan, C. A., Dombroski, A. J., and Platt, T. (1987) *Cell 48*, 945−952.
10. Walstrom, K. M., Dozono, J. M., Robic, S., and von Hippel, P. H. (1997) *Biochemistry 36*, 7980−7992.
11. Richardson, J. P., and Conaway, R. (1980) *Biochemistry 19*, 4293−4299.
12. Morgan, W. D., Bear, D. G., and von Hippel, P. H. (1984) *J. Biol. Chem. 259*, 8664−8671.
13. Andrew, C., and Richardson, J. P. (1985) *J. Biol. Chem. 260*, 5826−5831.
14. Geiselmann, J., Wang, Y., Seifried, S. E., and von Hippel, P. H. (1993) *Proc Natl. Acad. Sci. U.S.A. 90*, 7754−7778.
15. Reisbig, R. R., and Hearst, J. E. (1981) *Biochemistry 20*, 1907−1918.
16. Kassavetis, G. A., and Chamberlin, M. J. (1981) *J. Biol. Chem. 256*, 2777−2786.
17. Lau, L. F., Roberts, J. W., and Wu, R. (1983) *J. Biol. Chem. 258*, 9391−9397.
18. Morgan, W. D., Bear, D. G., and von Hippel, P. H. (1983) *J. Biol. Chem. 258*, 9565−9574.
19. Jin, D. J., Burgess, R. R., Richardson, J. P., and Gross, C. A. (1992) *Proc. Natl. Acad. Sci. U.S.A. 89*, 1453−1457.
20. Burova, E., Hung, S. C., Sagitov, V., Stitt, B. L., and Gottesman, M. E. (1995) *J. Bacteriol. 177*, 1388−1392.
21. Li, J., Mason, S. W., and Greenblatt, J. (1993) *Genes Dev. 7*, 161−172.
22. Nehrke, K. W., Zalatan, F., and Platt, T. (1993) *Gene Expression 3*, 119−133.
23. Farnham, P. J., Greenblatt, J., and Platt, T. (1982) *Cell 29*, 945−951.
24. Landick, R., and Yanofsky, C. (1984) *J. Biol. Chem. 259*, 11550−11555.
25. Wilson, K. S., and von Hippel, P. H. (1994) *J. Mol. Biol. 244*, 36−51.
26. Sigmund, C. D., and Morgan, E. A. (1988) *Biochemistry 27*, 5622−5627.
27. Guarente, L. P., Beckwith, J., Wu, A. M., and Platt, T. (1979) *J. Mol. Biol. 133*, 189−197.
28. Wu, A. M., Chapman, A. B., Platt, T., Guarente, L. P., and Beckwith, J. (1980) *Cell 19*, 829−836.
29. Wu, A. M., Christie, G. E., and Platt, T. (1981) *Proc. Natl. Acad. Sci. U.S.A. 78*, 2913−2917.
30. Galloway, J. L., and Platt, T. (1986) in *Regulation of Gene Expression*, 25 Years on Symposium of the Society for General Microbiology (Booth, I., and Higgins, C., Eds.) pp 155−178, Cambridge University Press, Cambridge, U.K.
31. Galloway, J. L., and Platt, T. (1988) *J. Biol. Chem. 263*, 1761−1767.
32. Zalatan, F., Galloway-Salvo, J., and Platt, T. (1993) *J. Biol. Chem. 268*, 17051−17056.
33. Platt, T. (1981) *Cell 24*, 10−23.
34. Mott, J. E., Galloway, J. L., and Platt, T. (1985) *EMBO J. 4*, 1887−1891.
35. Brennan, C. A., Steinmetz, E. J., Spear, P., and Platt, T. (1990) *J. Biol. Chem. 265*, 5440−5447.
36. Walstrom, K. M., Dozono, J. M., and von Hippel, P. H. (1997) *Biochemistry 36*, 7993−8004.

37. Chen, C.-Y. A., and Richardson, J. P. (1987) *J. Biol. Chem. 262*, 11292−11299.
38. Zhu, A. Q., and von Hippel, P. H. (1998) *Biochemistry 37*, 11215−11222.
39. Wilson, K. S., and von Hippel, P. H. (1995) *Proc. Natl. Acad. Sci. U.S.A. 92*, 8793−8797.
40. Lau, L. F., Roberts, J. W., and Wu, R. (1982) *Proc. Natl. Acad. Sci. U.S.A. 79*, 6171−6175.
41. Morgan, W. D., Bear, D. G., and von Hippel, P. H. (1983) *J. Biol. Chem. 258*, 9553−9564.
42. Richardson, L. V., and Richardson, J. P. (1996) *J. Biol. Chem. 271*, 21597−21603.
43. McSwiggen, J. R. (1987) Ph.D. Thesis, University of Oregon.
44. Bektesh, S. L., and Richardson, J. P. (1980) *Nature 283*, 102−104.
45. Chen, C.-Y. A., Galluppi, G. R., and Richardson, J. P. (1986) *Cell 26*, 1023−1028.
46. Zuker, M. (1989) *Science 244*, 48−52.
47. Van Gilst, M. R., Rees, W. A., Das, A., and von Hippel, P. H. (1997) *Biochemistry* 36, 1514−1524.

BI9729110